Fabrication of high aspect ratio 100 nm metallic stamps for nanoimprint lithography using proton beam writing

K. Ansari,[a] J. A. van Kan, A. A. Bettiol, and F. Watt
Center for Ion Beam Applications, Department of Physics, National University of Singapore, 2 Science Drive 3, Singapore 117542, Singapore

(Received 26 February 2004; accepted 21 May 2004)

We report a way of fabricating high-quality void-free high-aspect-ratio metallic stamps of 100 nm width and 2 μm depth, using the technique of proton beam writing coupled with electroplating using a nickel sulfamate solution. Proton beam writing is a one-step direct-write process with the ability to fabricate nanostructures with high-aspect-ratio vertical walls and smooth sides, and as such has ideal characteristics for three-dimensional (3D) stamp fabrication. Nanoindentation and atomic force microscopy measurements of the nickel surfaces of the fabricated stamp show a hardness and side-wall roughness of 5 GPa and 7 nm, respectively. The fabricated 100 nm 3D stamps have been used to transfer test patterns into poly(methylmethacrylate) films, spin coated onto a silicon substrate. Proton beam writing coupled with electroplating offers a process of high potential for the fabrication of high quality metallic 3D nanostamps. © *2004 American Institute of Physics*. [DOI: 10.1063/1.1773933]

Proton beam writing (PBW) has been demonstrated as a fast single step three dimensional (3D) direct write technique for fabrication of sub-100-nm-high aspect ratio structures in resists, with 30 nm resolution (potentially less), and less than 3 nm side wall roughness.[1] Direct-write processes for a long time have been considered intrinsically slow and inefficient compared with masked processes for the mass production of large-area high-density low-dimensional structures. However, the increased technical complexities and predicted increased cost of producing feature sizes smaller than 100 nm has called into question the traditional role of masked processes as the universal method of mass production. Direct write processes therefore may have some distinct advantages when used in combination with nanoimprinting.[2] Proton beam writing, which when combined with electroplating, provides a powerful fabrication process to create high quality metallic nanostamps. The fabricated stamps have potential applications in all the developed technologies based on molds and stamps.[2–10] PBW exhibits the following features: (a) the ability to fabricate structures with smooth and vertical side walls, which is crucial to minimize pattern distortion during demolding in nanoimprint lithography; (b) the ability to fabricate high aspect ratio sub-100-nm features in a one-step process; and (c) since proton beam writing exhibits minimal proximity effects, it is ideally suited to produce features of high packing density. The fabrication of metallic stamps with these combined characteristics is very difficult to achieve with other lithography techniques such as focused ion beam (FIB), electron beam lithography (EBL), optical or x-ray lithography. In this letter, we describe the fabrication of 100 nm high aspect ratio nickel stamps, which combines the advantages of PBW and traditional nickel electroplating.

PBW uses an accelerated focused beam of mega-electron-volt (MeV) protons to irradiate a positive resist such as poly(methymethacrylate) (PMMA) or a negative resist such as SU-8 (a chemically amplified, epoxy based resist). This technique is the proton beam analog of electron beam writing, where the main advantage of using protons as opposed to electrons is that protons have a straight, deep, well-defined path and range in polymers.[11] For MeV energetic protons incident on a resist material such as PMMA, the dominant energy loss mechanism is through electronic scattering. Protons, which have a mass of around 2000 times that of electrons, do not deviate as they travel through matter, and therefore maintain a straight path as they penetrate deep into the resist. Although the proton beam generates secondary electrons through radiation damage, the secondary electrons remain very close to the incident beam axis and therefore the proximity effect is much lower than for electron lithography.[12] 3D nanopatterns with vertical smooth sidewalls, high aspect ratio, and high feature densities can be fabricated using proton beam writing in a single step.

Similar to electron beam writing, the energy dissipated into the resist following exposure leads to chemical damage of the polymer bonds such as chain scissoring for positive resist and cross-linking in case of negative resist, which leaves behind a pattern in the resist after chemical development. Due to the efficient nature of the interaction, proton beam writing does not require specially developed amplified resists, which are necessary in deep ultraviolet (DUV) and extreme ultraviolet (EUV) nanolithography. PBW as a process is physically different from the relatively slow FIB, which uses heavy ions to sputter atoms from the surface of the material. Conventional FIB has a material removal rate of 1–10 atoms per incident ion, which is approximately one million times less efficient than the removal rate per incident proton for proton beam writing, although the advantage of FIB is that it does not require a resist and can be used on a variety of materials.

A schematic representation of the process of stamp fabrication using proton beam writing is shown in Fig. 1. This process involves: (a) Coating a conductive seed layer for electroplating onto a Si substrate followed by a spin coated layer of resist, e.g., PMMA, and exposure using proton beam writing, (b) deposition of a second metallization layer on the top surface which acts as a seed layer for the base of the

[a]Electronic mail: phyamk@nus.edu.sg

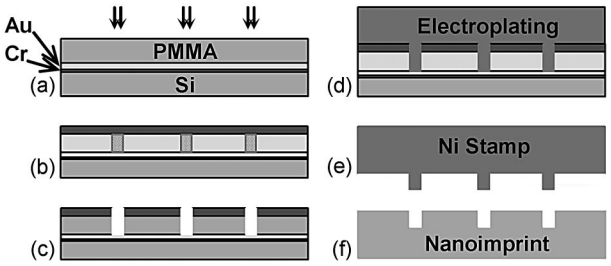

FIG. 1. Schematic representation of the process of stamp fabrication using proton beam writing.

stamp, (c) development of the structures, (d) electroplating of the structures, plus overplating to form the base for the stamp, (e) delamination of the stamp from the substrate, and (f) nanoimprinting. The fabrication process was started by coating a clean 3 in. Si wafer by, consecutively, 20 nm Cr followed by 200 nm Au using e-beam evaporation. This coating ensures adhesion as well as electrical conductivity for the electrodeposition step. The Au(200 nm)/Cr(20 nm)/Si (100) coated wafers were cleaned with acetone, rinsed with DI water, dried, and prebaked at 250 °C for 1 *h* to dehydrate the surface thereby ensuring good adhesion prior to coating with resist. A layer of 2 μm PMMA 950 000 molecular weight (MW), 11 wt % in anisole, was spin coated onto the wafers, and baked at 180 °C for 30 min. The lithographic patterning was carried out using the P-Beam writing facility at the National University of Singapore.[13,14] Here, a beam of 2 MeV protons was focused to a spot size of 60×90 nm^2 and magnetically scanned over an area of 50×50 μm^2. The test pattern, a precursor to a microfluidic lab-on-a-chip system, consisted of 100 nm parallel trenches connected to reservoirs of 50 μm (width) $\times$ 500 μm (length). Since the range of a 2 MeV proton is around 60 μm, the protons penetrate through the resist into the silicon substrate, and so the depth of the structures is determined by the thickness of the resist, which in this case is 2 μm.

Due to the small dimensions and high aspect ratios of the channels, we used a less viscous developer than normal to enable rapid diffusion of the developer into the structures. For these high aspect ratio narrow structures, IPA-water (7:3) developer at room temperature was used for 20 min in steps of 2 min developing 30 s rinse in deionized water to drive out the exposed resists. This change in development procedure required an adjustment in the proton exposure: The normal proton exposure dose of (80 nC/mm^2),[1] which is the optimal value for the more viscous widely used GG developer, was for this case adjusted to 200 nC/mm^2.

The plating has been carried out using a typical Ni sulfamate bath solution with sodium-dodecyl-ether-sulphate wetting agent and without organic additives using a Technotrans AG, RD.50 plating system. The deposition is carried out employing first a low current density of 0.4 A/dm^2, which leads to a growth rate of 100 nm/min for the first 50 μm and a high current density of 4 A/dm^2, equivalent to a growth rate of 1 μm/min for the next 200 μm. The initial low plating current density produces less intrinsic stress in the high aspect ratio structures, and is also coupled with the highest hardness. After delamination, the stamps were cleaned in toluene at 40 °C for 30 min. Figure 2 shows a series of electron microscope photographs, which shows the test

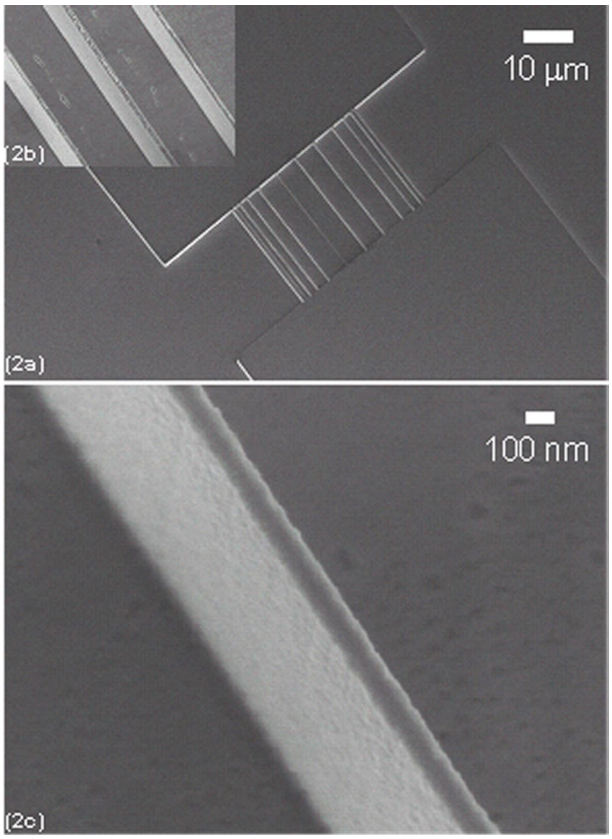

FIG. 2. (a) Low magnification SEM image of a nickel stamp fabricated using proton beam writing and nickel electroplating. The stamp is a test pattern featuring two raised platforms connected by several 100 nm wide $\times 2$ μm (depth) $\times$ 30 μm (length) high aspect ratio ridges. This test pattern will be used to imprint a microfluidic lab-on-a-chip system featuring two reservoirs and a series of connecting 100 nm channels (b) SEM image showing three of the connecting 100 nm Ni stamp ridges, and (c) a high magnification picture of one Ni ridge, exhibiting vertical sidewalls, and a smooth surface (7 nm).

stamp including the fabricated metallic Ni ridges of 100 nm width and 2 μm height.

Initially we had a problem with the appearance of voids in the plated high aspect ratio ridges on the stamp. In the first process we tried, the second metallization procedure (which is needed for overplating to form the stamp base) followed proton beam writing and development. In this case however, during the second metallization process, slight deposition of the metal ions occurred on the side walls of the developed structures. This deposition resulted in electric contact between the top metallic layer and the bottom seed layer. As a consequence, during the plating step, metal was plated on the side wall which for high aspect ratio structures can block the trench thereby forming a void. To eliminate side wall electroplating, thereby eliminating voids, two approaches have been explored: (1) deposition of the second metallization layer before proton beam patterning; this relies on the proton beam penetrating the second metallization layer without adverse effects and (2) deposition of the second metallization layer after proton exposure, but before developing the exposed areas. Both methods rely on the penetration of the developer through the second metallization layer, which has good adhesion to the resist. This layer should be thin enough to develop the structures but thick enough to provide a conductive layer for the subsequent over-plating process. Our experimental results show that deposition of a second metal-

lization layer of 3 nm Ti provides adequate adhesion and good conductivity. Both processes outlined above were able to completely eliminate the voids.

Nanoindentation and atomic force microscopy (AFM) measurements have been used to characterize the hardness and the side wall roughness of the stamps, respectively. Due to the small dimensions of the ridges, nanoindentation measurements were performed away from the stamp ridges over an adjacent area of $100\times100\ \mu m^2$, using UMIS-2000H nanoindenter with a Berkovich indenter tip. Hardness and Young's modulus of 5 and 213 GPa were obtained respectively which is consistent with the previously reported values.[15] The side wall roughness and the side wall angles are two important factors affecting the imprinting process. Calculations and previous measurements indicate a side wall angle of better than 89.5 deg for proton beam writing.[16] In order to determine the surface roughness of the side walls of the plated structures, a $50\times50\ \mu m^2$ area of 50-μm-thick negative Su-8 resist spun on Si\Cr(20 nm)\Au(200 nm) was irradiated by a 2 MeV proton beam. After developing of the unexposed areas, the structure was plated using the conditions above, and the remainder of the Su-8 was removed. The structure was fabricated over the edge of the wafer so that after removing the exposed Su-8, the plated sidewall is accessible from the side of the sample. A surface roughness of 7 nm was measured over an area of $2\times2\ \mu m^2$ by AFM using a Nanoscope III (Digital Instruments) equipped with a silicon tip and operating in the tapping mode.

Nanoimprinting was carried out with a commercial nanoimprinter (Obducat Technologies AB, NIL-2-PL 2.5 in. nanoimprinter) using 8-μm-thick PMMA resist 950 000 (11 wt %) in anisole double spin coated on Cu(200 nm)/Ti(20 nm)/Si substrate. The Cu is deposited to aid adhesion of the PMMA to the substrate.[17] NIL was carried out using the masters directly without any treatment with antiadhesion agent. The imprinting cycle consists of: 5 min at 190 °C and 50 bar, followed by 20 s at 170 °C and 20 bar. The pressure was released after cooling just below 110 °C. Empirical results show that the second part of the cooling down cycle effectively prevents the pattern's shifting after imprinting. One possible explanation for this is that since according to our experimental results, at low pressures such as 20 bar or less imprinting is incomplete even if the temperature is high, pressures as low as 20 bar or less has minimal pattern distortion. Consequently, the gradual release of the stamp at these low pressures during the cooling down procedure ensures minimal movement between the stamp and the mold without pattern distortion. However, further investigation is necessary to fully understand this process. Upon separation of the stamp from the substrate, no peeling off was observed, and the stamp patterns were transferred into the PMMA resist. An electron micrograph of the imprinted pattern is shown in Fig. 3. The replicated pattern had vertical sidewalls and flat surfaces identical to the stamp.

In conclusion, we have demonstrated a way of making 3D stamps. Proton Beam Writing together with traditional electroplating can be used as a powerful fabrication process for mould, stamp, and 3D mask technology. Metallic stamps with 100-nm-straight-sided high aspect ratio (~20) features, 7-nm-side-wall roughness, and precise geometry have been realized and transferred into polymer using nanoimprint lithography.

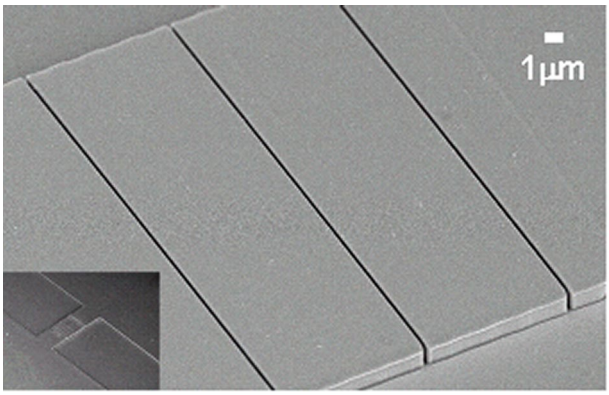

FIG. 3. Imprint of the Ni stamp in 8 μm thick PMMA spin coated on a silicon substrate, showing reproducible fine features, smooth sidewalls, and vertical structures. Inset: low magnification view of the imprint.

The authors would like to acknowledge financial support from ASTAR (Singapore), the NUS for providing a scholarship for K.A., and the Singapore Institute of Manufacturing Technology (SIMTech) for top-up support.

[1] J. A. van Kan, A. A. Bettiol, and F. Watt, Appl. Phys. Lett. **83**, 1629 (2003).
[2] S. Y. Chou, P. R. Krauss, and P. J. Renstrom, Appl. Phys. Lett. **67**, 3114 (1995).
[3] X. M. Zhao, Y. Xia, and G. M. Whitesides, Adv. Mater. (Weinheim, Ger.) **8**, 837 (1996).
[4] A. Kumar and G. M. Whitesides, Appl. Phys. Lett. **63**, 2002 (1993).
[5] E. Kim, Y. Xia, and G. M. Whitesides, Nature (London) **376**, 581 (1995).
[6] J. L. Wilbur, A. Kumar, H. A. Biebuyck, E. Kim, and G. M. Whitesides, Nanotechnology **7**, 452 (1996).
[7] Y. Xia and G. M. Whitesides, Angew. Chem., Int. Ed. Engl. **37**, 550 (1998).
[8] E. Schaffer, T. Thurn-Albrecht, T. P. Russell, and U. Steiner, Nature (London) **403**, 24 (2000).
[9] N. Stutzmann, T. A. Tervoort, K. Bastiaansen, and P. Smith, Nature (London) **407**, 613 (2000).
[10] Q. Xia, C. Keimel, H. Ge, Z. Yu, W. Wu, and S. Y. Chou, Appl. Phys. Lett. **83**, 2 (2003).
[11] J. A. van Kan, T. C. Sum, T. Osipowicz, and F. Watt, Nucl. Instrum. Methods Phys. Res. B **161**, 366 (2000).
[12] H. J. Whitlow, M. L. Ng, V. Auzelyte, I. Maximov, L. Montelius, J. A. van Kan, A. A. Bettiol, and F. Watt, Nanotechnology **15**, 223 (2004).
[13] J. A. van Kan, A. A. Bettiol, and F. Watt, Mater. Res. Soc. Symp. Proc. **777**, T2.1.1 (2003).
[14] F. Watt, J. A. van Kan, I. Rajta, A. A. Bettiol, T. F. Choo, M. B. H. Breese, and T. Osipowicz, Nucl. Instrum. Methods Phys. Res. B **210**, 14 (2003).
[15] T. Fritz, W. Mokwa, and U. Schnakenberg, Electrochim. Acta **47**, 55 (2001).
[16] J. A. van Kan, A. A. Bettiol, and F. Watt, Nucl. Instrum. Methods Phys. Res. B **181**, 258 (2001).
[17] V. K. P. Kanigicherla, K. W. Kelly, E. Ma, W. Wang, and M. C. Murphy, Microsyst. Technol. **4**, 77 (1998).